



High linear regioselectivity in the rhodium-catalyzed hydro(deuterio)formylation of 3,4,4-trimethylpent-1-ene: The role of β -hydride elimination

Raffaello Lazzaroni^{a,*}, Roberta Settambolo^b, Giuliano Alagona^{c,**}, Caterina Ghio^c

^a DCCI, University of Pisa, Via Risorgimento 35, I-56126 Pisa, Italy

^b CNR-ICCOM, Pisa UOS, Via Risorgimento 35, I-56126 Pisa, Italy

^c CNR-IPCF, Pisa UOS, Molecular Modeling Lab, Via Moruzzi 1, I-56124 Pisa, Italy

ARTICLE INFO

Article history:

Received 21 July 2011

Received in revised form

26 November 2011

Accepted 18 December 2011

Available online 27 December 2011

Keywords:

Hydroformylation

Deuterioformylation

DFT

B3P86/6-31G*

ECP/LanL2DZ

Regioselectivity

3-Methylbut-1-ene

3-Methylpent-1-ene

3,4-Dimethylpent-1-ene

3,4,4-Trimethylpent-1-ene

ABSTRACT

The regioselectivity in the hydroformylation reaction catalyzed by an unmodified Rh catalyst has been investigated for a number of α -methylsubstituted alk-1-enes (3-methylbut-1-ene **MB**₁, 3-methylpent-1-ene **MP**₁, 3,4-dimethylpent-1-ene **DMP**₁, and 3,4,4-trimethylpent-1-ene **TMP**₁) experimentally (at 20 °C and 100 atm CO/H₂ total pressure) and theoretically at the B3P86/6-31G* level with Rh described by effective core potentials in the LanL2DZ valence basis set. For all substrates the formation of the linear aldehyde (L) with respect to the branched one (B) in a prevailing amount has been observed (L/B > 62/38); the L isomer was formed as the almost exclusive product in the case of **TMP**₁ (L/B = 95/5). ²H NMR investigations of crude reaction mixtures, coming from analogous deuterioformylation experiments interrupted at partial substrate conversion, showed that in the case of **TMP**₁ only the branched alkyl-rhodium intermediate, precursor of the branched aldehyde, via β -hydride elimination mainly generates terminal deuterated olefins and, to a lesser extent, internal ones. The reversibility of the branched alkyl-Rh intermediates accounts for the high regioselectivity in favor of the linear aldehyde. Computational studies confirm the importance of the alkyl-Rh transition state (TS) stability to reproduce the experimental regioselectivity, or even to predict it, when the reaction is nonreversible (i.e. for **MB**₁, **MP**₁, and **DMP**₁). In the case of **TMP**₁, the free energy profiles for further reaction steps along branched and linear pathways have been examined to elucidate the origin of reaction reversibility. The TS for the alkyl migratory insertion onto the CO coordinated to rhodium, higher than that for the alkyl-Rh intermediate formation, explains the reason why in deuterioformylation experiments at partial conversion the monodeuterated terminal olefin **TMP**₁-1-d₁ is obtained. This occurs for one out of two most populated reactant conformers of **TMP**₁, although for the Curtin–Hammett principle reactant populations are not particularly important. For the other, the reaction proceeds to the branched aldehyde. Only for a less populated reactant conformer the internal olefin is obtained. Conversely, along the linear pathway the CO addition and alkyl migratory insertion steps occur, respectively, in a practically spontaneous way and with very low TS in any case. Agostic interactions (using the QTAIM theory) and kinetic isotope effects have been evaluated and discussed. The examination of further reaction steps for **DMP**₁ allowed us to demonstrate that the reaction is nonreversible for that substrate, despite the similarity between **DMP**₁ and **TMP**₁. The *tert*-butyl group exerts its steric hindrance mainly on the very first branched reaction steps, favoring an alkyl-Rh TS arrangement lower in free energy than the alkyl-Rh migratory insertion onto the coordinated CO. In part the branched material returns to the reactant complex, thus enriching the linear fraction.

© 2011 Elsevier B.V. All rights reserved.

1. Introduction

Under rhodium-catalyzed hydroformylation conditions, the alkene insertion into the Rh–H bond, which gives rise to the

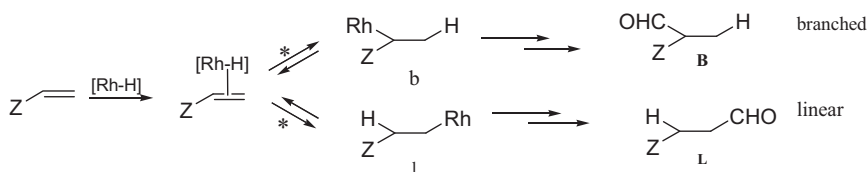
alkyl-metal intermediates along the pathway to the linear, L, or branched, B, product aldehydes (Scheme 1), can be a reversible or nonreversible step, primarily depending on the temperature and the substrate nature.

We found that at 100 °C β -hydride elimination occurs for various vinyl substrates such as ethyl vinyl ether, 1-hexene, allyl ethyl ether, styrene and other aromatic substrates. While for aliphatic vinyl [1] and allyl alkenes [1–3] β -hydride elimination involves both the linear and branched alkyl intermediates, for the aromatic substrates (styrene) it occurs primarily for the branched ones [4–9]. By contrast, at low temperature (<25 °C), these substrates do

* Corresponding author at: DCCI, University of Pisa, Via Risorgimento 35, I-56126 Pisa, Italy. Tel.: +39 0502219 227; fax: +39 0502219 260.

** Corresponding author at: CNR-IPCF, Pisa UOS, Molecular Modeling Lab, Via Moruzzi 1, I-56124 Pisa, Italy. Tel.: +39 050315 2450; fax: +39 050315 2442.

E-mail addresses: lazza@dcci.unipi.it (R. Lazzaroni), G.Alagona@ipcf.cnr.it, G.Alagona@pi.ipcf.cnr.it (G. Alagona).



Scheme 1. Regioselectivity in the hydroformylation reaction of a terminal olefin. * Reversibility depending on the temperature and the substrate nature.

Table 1
Regioselectivity values for the hydroformylation of α -methylsubstituted alk-1-enes under 20 °C and 100 atm CO/H₂ (1:1), at partial (20%) and complete substrate conversion.

1	R	L:B (20% conv.)		L:B (complete conversion)	
		Experimental data	Computational results ^a	Experimental data	Computational results ^a
				ΔE	ΔG
MB₁	Me	63:37	62:38	62:38	62:38
MP₁	Et	67:33	66:34	62:38	66:34
DMP₁	<i>i</i> -Pr	74:26	72:28	58:42	68:32
TMP₁	<i>t</i> -Bu	96:4	95:5	53:47	85:15

^aB3P86/6-31G*/Lan12DZ L:B ratios based on either potential (ΔE) or free (ΔG) energies.

not give β -hydride elimination and thus the alkyl formation is a nonreversible step determining the regioselectivity of the process. In order to establish whether the alkyl formation is a reversible step at low temperature also for vinyl substrates bearing a bulky substituent in α position with respect to the double bond, some 3-alkyl substituted alk-1-enes (see Table 1 for their definition) were hydroformylated by us. Four different R moieties were taken into account: they are in turn the methyl (Me), ethyl (Et), *iso*-propyl (*i*Pr), and *tert*-butyl (*t*Bu) groups, leading respectively to 3-methylbut-1-ene (**MB₁**), 3-methylpent-1-ene (**MP₁**), 3,4-dimethylpent-1-ene (**DMP₁**), and 3,4,4-trimethylpent-1-ene (**TMP₁**).¹

Deuterioformylation runs carried out under the same hydroformylation conditions, at partial substrate conversion, were exploited to elucidate the chemical behavior of the 1-alkenes taken into account. In particular, deuterioformylations at partial substrate conversion of the substrate bring out significant information on the possible reaction reversibility in the alkyl formation, as previously remarked in the literature also by other authors for the hydroformylation of a variety of substrates employing different catalytic precursors [10–12].

From a computational view-point, in the absence of β -hydride elimination, the regioselectivity of the reaction can be evaluated on the basis of the potential or free energy of the isomeric alkyl formation, provided all the possible conformers are taken into account, and compared with the regioselectivity of aldehyde formation [13]. Conversely, when the reaction is reversible, the subsequent reaction steps need to be examined with theoretical calculations at the free energy level [14] (refer to the Computational Details section for a description of employed methods) to investigate and eventually rationalize the origin of reversibility. Kinetic isotope effects (KIE) [15] have also been evaluated as well as the agostic interaction in the alkyl-tricarbonyl intermediates in terms of the QTAIM theory [16].

¹ Apart the first substrate (**MB₁**), the others bear a chiral group. Both enantiomers (indicated using a plain or a primed name) need to be computed to consider the attack onto either face of the double bond as well as that the chiral substrates are used in racemic form in the experiments.

2. Results and discussion

2.1. Hydroformylation

Hydroformylation of the alk-1-enes (Table 1) was carried out in benzene both at partial and complete substrate conversion in a stainless-steel autoclave with Rh₄(CO)₁₂ as catalyst precursor, at room temperature, under 100 atm total pressure (CO/H₂ = 1:1). The composition of the reaction mixtures was evaluated by GC analysis, using *n*-decane as the internal standard.

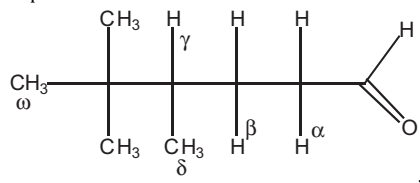
In the case of the simplest olefins (**MB₁** and **MP₁**) a slight L-regioselectivity occurs, the L:B molar ratio varying from 62:38 to 66:34 both at partial and total substrate conversion. A larger prevalence of the L isomer (L:B = 72:28) was observed in the case of **DMP₁** bearing an *i*Pr group at C₃. The regioselectivity turns out to be almost exclusively in favor of the L-regioisomer with **TMP₁**, a substrate characterized by the presence of a *t*-butyl group in α position with respect to the double bond.

2.2. Deuterioformylation

In order to establish if the Rh-alkyl formation is or not a reversible step of the reaction, deuterioformylation experiments with the above substrates were carried out. The same approach had been previously employed with the same purpose by Casey and Petrovich [10] and Nozaki et al. [12] among the authors here cited. In the case of **TMP₁**, the runs were carried out at both partial and total conversion, at 20 °C under 100 atm of CO and D₂ (1/1) at constant pressure. The reaction was stopped after about 40 min at 20% substrate conversion into aldehydes. The reaction mixture was also examined after 3 h at complete substrate conversion.

At the two selected conversion degrees (20% and total conversion), samples of the reaction mixtures, containing unconverted olefins and products, were directly analyzed without any handling or treatment. The regioselectivity was high and, as in the hydroformylation, in favor of the linear aldehyde. Inspection of the ²H NMR spectra allowed rapid and complete identification of all deuterated species present in solution. The ²H NMR resonances were assigned by comparison with the analogous signals present

Table 2
 ^1H NMR chemical shifts (δ , ppm) of species arising from hydroformylation of **TMP**₁ at partial substrate conversion.



Proton type	Signal	δ (ppm)	
		$\text{C}_6\text{H}_6^{\text{a}}$	CDCl_3^{b}
α	2 Multiplets	1.9 and 1.75	2.4 and 2.28
γ	Multiplet	1.62	1.82
β	Multiplet	0.81	1.1
δ	Doublet	0.55	0.84
ω	Singlet	0.7	0.8

^a Reaction solvent.

^b After removal of benzene.

in the ^1H NMR spectra (solvent C_6D_6) of the corresponding hydroformylation mixtures (the chemical shifts obtained are reported in Table 2).

It is worth noting that the values in benzene as a solvent are quite different from the values obtained in CDCl_3 . In particular, the chemical shifts of the L isomer for the CH_2 in β position with respect to the formyl group are 0.81 in benzene and 1.1 ppm in CDCl_3 .

In the ^2H NMR spectrum relative to deuterioformylation experiments at 20% conversion (Fig. 1 and Table 3), the two signals at 9.32 and 0.80 ppm are due to the deuterium atom of the formyl group into **L-1,3-*d*₂** and **L-1-*d*₁** aldehydes and to the deuterium atom on the carbon in β -position into **L-1,3-*d*₂** one, respectively. The intensity of the formyl group signal is higher than that of the deuterium in β -position with a ratio of 1:0.65 (*vide infra* for a discussion).

The sample also shows a significant resonance at 4.93 ppm which can be assigned to a deuterium atom bonded to the terminal carbon atom of the unconverted olefin **TMP**₁-**1-*d*₁**. In addition, while the signal at 1.49 ppm is likely due to a deuterium atom bonded to the terminal carbon atom of 3,4,4-trimethylpent-2-ene (**TMP**₂-**1-*d*₁**), the signal at 1.602 ppm can be assigned to the deuterium atom CHDCDO in α position to the carbonyl group arising from deuterioformylation of the substrate monodeuterated in terminal position **TMP**₁-**1-*d*₁** (**L-1,2,3-*d*₃**).

The GC–MS spectra, in addition to the unconverted substrate, show the presence of isomerized olefins. No traces of hydrogenation products were observed.

The formation of deuterated olefins under deuterioformylation conditions can be reasonably explained taking into account the reversible formation of the tertiary alkyl-metal intermediate as

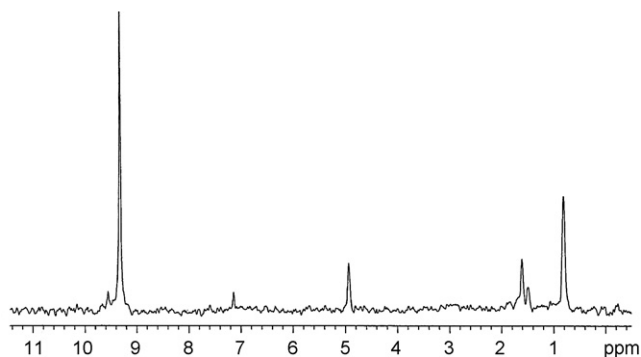


Fig. 1. ^2H NMR spectrum (46 MHz, 25 °C, C_6D_6 as external standard) of the crude reaction mixture obtained by deuterioformylation of **TMP**₁ at 20% substrate conversion.

well as the isotopic effect that favors the Rh–H elimination with respect to the Rh–D one [15c].

As reported in Scheme 2, in the light of the generally accepted mechanism of the hydroformylation reaction, the branched alkyl-rhodium intermediate (b) gives, via β -hydride elimination, the complex between the deuterated olefins **TMP**₁-**1-*d*₁** and Rh–H. Exchange of labeled olefins with unlabeled **TMP**₁ gives the non-deuterated η^2 -**TMP**₁ complex and the free deuterated terminal olefins. The same alkyl can also undergo β -elimination to give the internal olefin **TMP**₂-**1-*d*₁**. It is known that the β -hydride elimination is controlled by a kinetic isotope effect [15c], which means that elimination of Rh–H is faster than that of Rh–D; this effect could account for the observed accumulation of deuterated species in the unconverted substrate.

Only in part the branched alkyl gives, via the normal hydroformylation steps, a small amount (5%) of the branched aldehyde. Conversely, no β -elimination occurs for the linear alkyl (l) (no terminal olefin deuterated at C2 of the double bond was observed), while it completely evolves into the corresponding L aldehyde.

The η^2 -**TMP**₁ complex brings about the monodeuterated aldehyde without D in β -position (**L-1-*d*₁**) (Scheme 2 and Table 3). This accounts for the intensity of the CDO signal higher than that of the D in β -position.

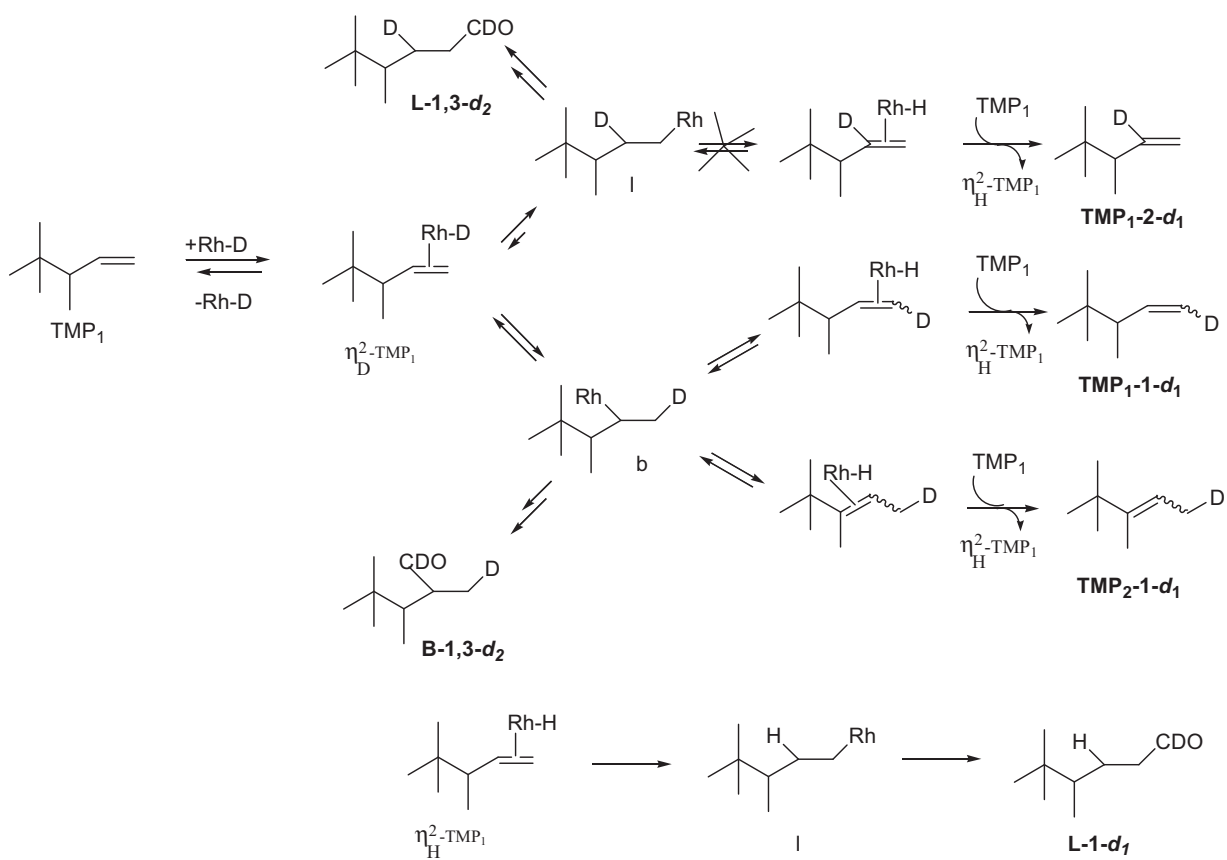
Deuterioformylation of **DMP**₁ was also carried out under the same experimental conditions adopted for **TMP**₁. A regioselectivity ratio (L/B) of 72/28 was observed, such as a value similar to that found for hydroformylation. ^2H NMR spectrum of a sample of the crude reaction mixture recovered at 20% substrate conversion shows the presence of the signal due to CDO and the resonances for CHD of the linear aldehyde and CH_2D of the branched isomer respectively. No traces of terminal or internal olefin deuterated in terminal position have been observed. An accurate analysis of GC and GC–MS showed the presence of a small amount (less than 5%) of isomerized olefins.

It is noteworthy that for the simplest substrates, i.e. **MB**₁ and **MP**₁, β -hydride elimination does not occur and only two signals for the linear aldehyde and two signals for the branched one were observed in ^2H NMR spectra.

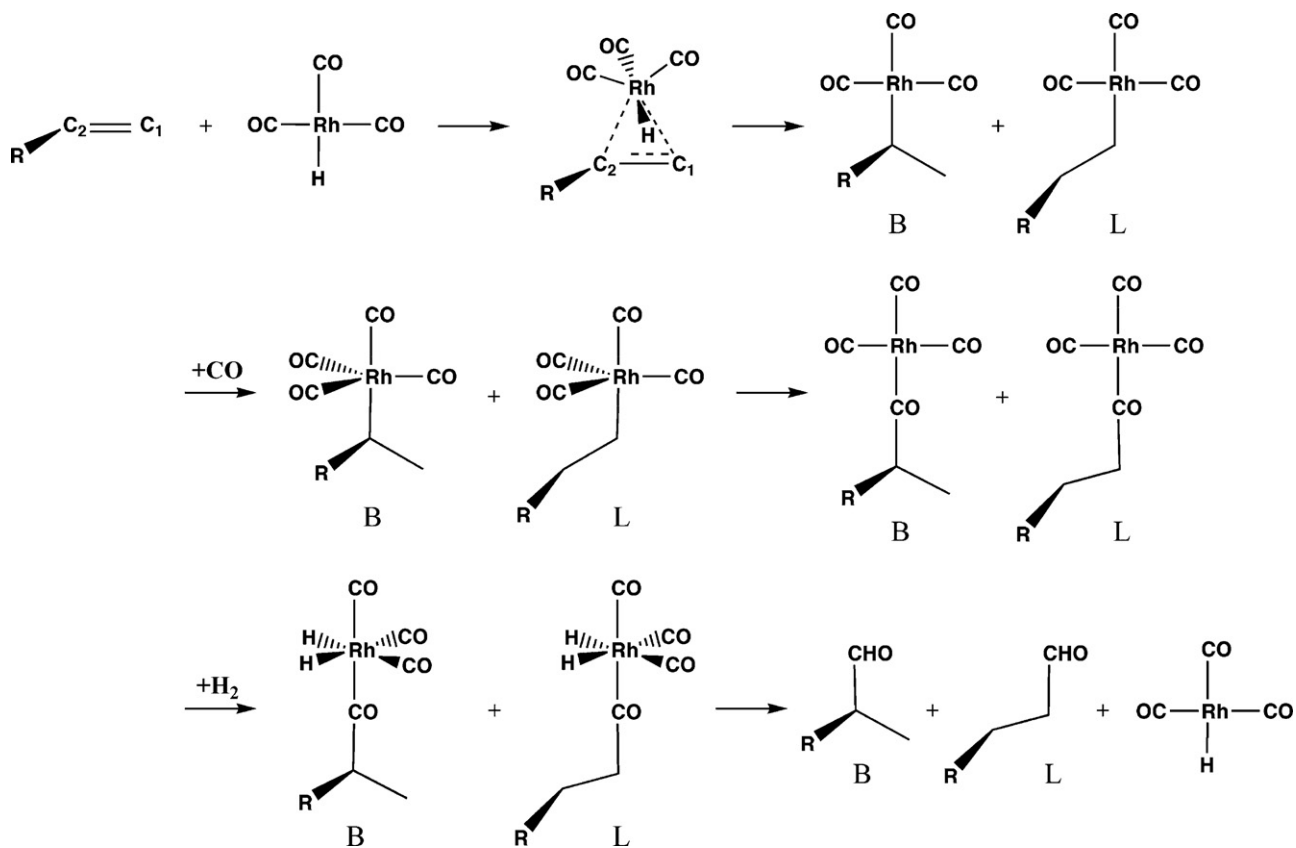
In order to explain the observed linear regioselectivity, the electronic effect of the R group could be taken in account, the +I influence of the *t*-butyl group being stronger than those of *i*-Pr and Me. Nevertheless, the steric hindrance is mainly responsible for the β -elimination. In particular the bulky *t*-butyl group in **TMP**₁, depending on its arrangement, can hamper the evolution of the branched alkyl to the corresponding branched aldehyde and favor β -hydride elimination. For the other branched alkyls, the steric effect exerted by a *sec*-alkyl group bonded to the vinyl group accounts for the prevalence of the linear isomer with respect to the branched one, the steric hindrance being not enough to determine β -hydride elimination. Thus, with **TMP**₁, unlike what observed for all vinyl olefins previously investigated [1–3], β -hydride elimination at room temperature occurs, and exclusively for the branched alkyl intermediate.

2.3. Theoretical investigations on β -hydride elimination

Theoretical regioselectivities computed under the hypothesis of nonreversibility reproduce the experimental ratios at complete conversion (Table 1) exactly for **MB**₁ and almost exactly for **MP**₁ when the potential energy-based values, also reported in Table 1 (fifth column), are used, as earlier found for other substrates [13] as well. When Et is replaced with either an *i*-Pr (**DMP**₁) or a *t*-Bu (**TMP**₁) group, theoretical ratio underestimates with respect to the experimental values turn out to be increasingly more evident (58:42 vs. 72:28 and 53:47 vs. 95:5) unlike for the other substrates. Interestingly enough, when free energy-based values [14], also



Scheme 2. Regioselectivity in the deuteroformylation reaction of TMP_1 .



Scheme 3. Mechanism of hydroformylation proposed by Wilkinson et al. [35] for a terminal olefin.

Table 3²H NMR chemical shifts (δ , ppm)^a of deuterated species arising from deuterioformylation of **TMP**₁ at partial substrate conversion.

SPECIES					
δ	4.93	1.49	0.80	9.32	1.60

^a Referred to C₆D₆ as external standard; 46 MHz, C₆H₆, 25 °C.

reported in Table 1 (last column), are used, theoretical results for the alkyl-Rh TS exactly reproduce the experimental ratios for **MB**₁ and **MP**₁, while for **DMP**₁ the calculated ratio (68:32) turns out to be in quite good agreement with the experiment. Actually, even for **TMP**₁ the regioselectivity evaluated employing free energy-based results (L:B=85:15) is satisfactory, being just slightly underestimated with respect to the experimental value (L:B=95:5). Anyway, the experimental evidence of β -hydride elimination in the case of **TMP**₁ prompted us to theoretically investigate the subsequent reaction steps (Scheme 3) to elucidate and possibly rationalize the origin of reaction reversibility. To this end, all the stationary points need to be located on the potential energy surface and their free energies need to be computed because of the change in the number of species along the reaction pathways. Primarily the fourth CO approaching path that played a critical role in 1,1-diphenylethene [17,18], and the TS for the alkyl migratory insertion onto the coordinated CO, have been considered. Although along the branched profiles for the addition of the fourth CO group to the alkyl-Rh tricarbonyl intermediates there are remarkably high barriers (see Fig. 2 and Section 2.3.2), unlike for the linear profiles [19] discussed below, the alkyl migratory insertion TS are higher in any case than the CO addition ones. Therefore, in what follows, the CO addition

TS are disregarded when comparing the TS relative free energies, but not when the reaction profiles are plotted.

Conformer names are 0, 1, 2 if the H₂CCH₃ value (Fig. 3) is roughly trans (t), gauche⁺ (g), gauche⁻ (g'). Both enantiomers have been considered for chiral substrates (four reactant intermediate structures are reported in Fig. S1 of Electronic Supporting Information (ESI)).

In one of the branched pathway profiles for **TMP**₁ (Fig. 2), the migratory insertion of the alkyl onto the coordinated CO leads to a CO insertion TS higher than the alkyl-Rh TS (13.24 and 10.88 kcal/mol, respectively). Therefore the reaction proceeds to the left, via β -hydride elimination, returning to the initial reactant intermediate (Reac Int), which corresponds to the monodeuterated terminal olefin **TMP**₁-1-*d*₁ found in the deuterioformylation experiment at partial conversion. This occurs for one of the most stable reactant complexes (named Reac0) taken as zero. The conformer stability for intermediates should be a minor detail provided their interconversion barriers are lower than the reaction TS according to the Curtin–Hammett principle [20]. Conversely, in this case, neither Reac2 (the reactant intermediate corresponding to the B2 alkyl-Rh(CO)₃ intermediate) nor the corresponding alkyl-Rh TS could be located despite several attempts making use of constrained

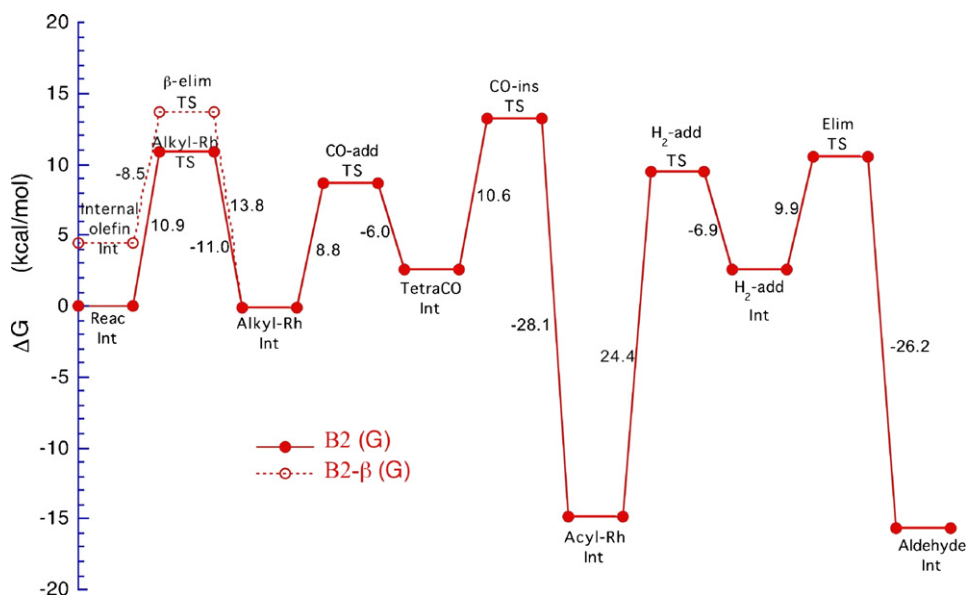


Fig. 2. Free energy profile along one of the branched pathways for **TMP**₁ (0-B2). The β -elimination TS leading to the internal olefin is drawn with dotted lines and empty markers.

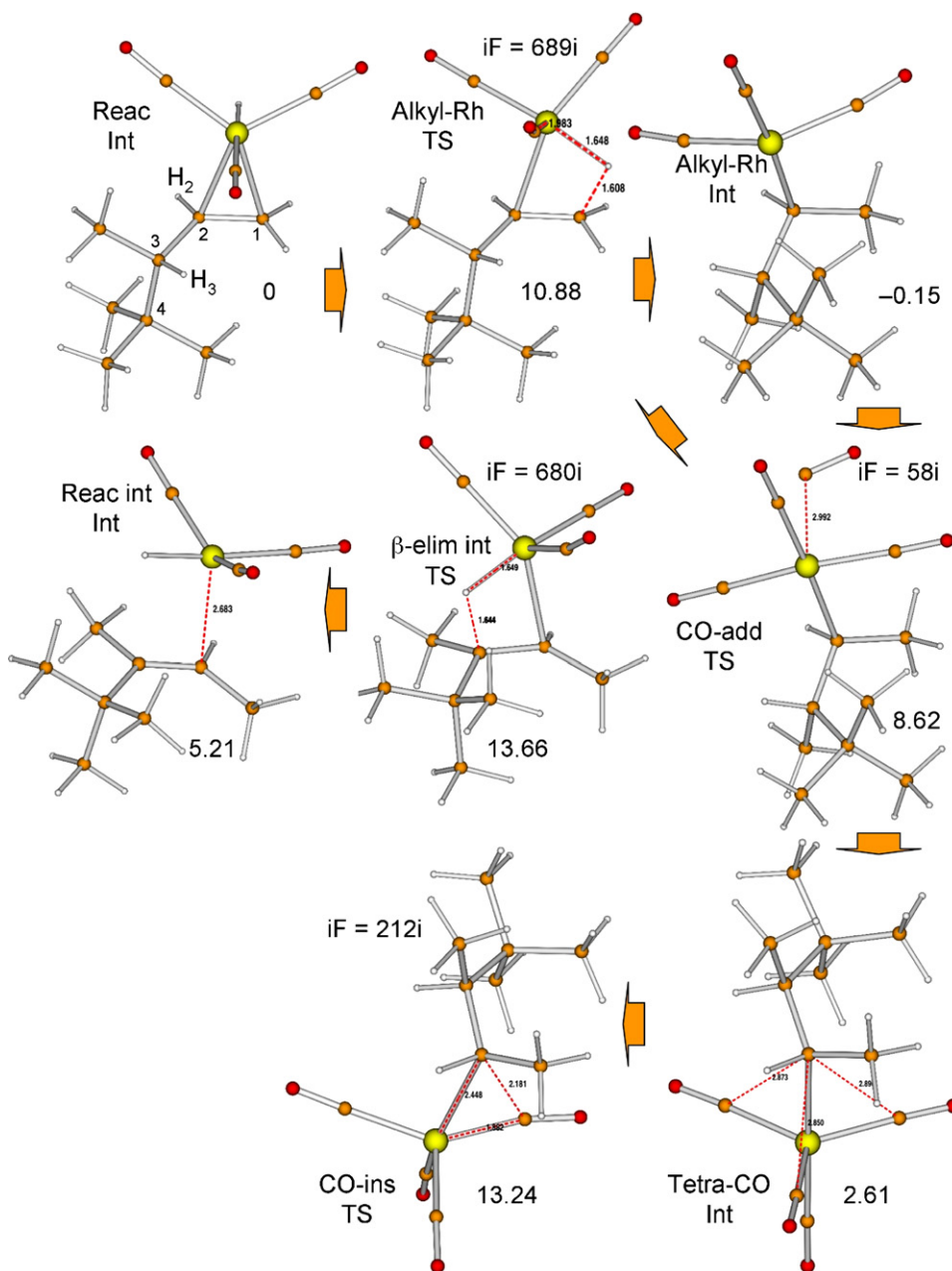


Fig. 3. Structures of the stationary points along the branched pathway for 0-B2 in Fig. 2. Their relative free energies (kcal/mol) and the TS imaginary frequencies (cm^{-1}) are also reported.

optimizations [19]. Interestingly, following the reaction pathway backwards starting from the B2 alkyl-Rh(CO)₃ intermediate, the B0 alkyl-Rh TS was obtained yielding React0, i.e. the most stable reactant intermediate. This means also that when the B0 alkyl-Rh TS is reached there are at least two competing branched pathways leading to either the B0 or B2 alkyl-Rh(CO)₃ intermediate. This is the reason why in the legend of Fig. 2 the involved conformer has been indicated as 0-B2. In this case the internal olefin cannot be obtained, again via β -hydride elimination, because the TS for its formation, also displayed in Fig. 2 (dotted line) for comparison, is higher (13.66 kcal/mol) and thus less favorable than both alkyl-Rh and CO insertion TS. Stationary-point structures through the CO-insertion TS are displayed in Fig. 3.

Interestingly enough, β -hydride elimination to yield the internal olefin occurs along the B'0 pathway for one of the reactant complex considered (React'0).

The hydroformylation reaction for **TMP**₁ is actually non-reversible for React0 along the B0 pathway producing the corresponding aldehyde, as occurs along the linear pathways for all reactant complexes (one of the linear profiles is displayed in Fig. 4²: once the rate-limiting step, i.e. the alkyl-Rh TS, is crossed, the reaction proceeds by formation of products).

Thus, from a computational view-point, the branched alkyl in part produces again the starting olefin that reacts with the same regioselectivity as before explaining the further increase in the linear fraction, and in part produces the branched aldehyde.

² All the TS and intermediates along the profile are displayed for clarity, although for Curtin–Hammett systems “theoretical calculation of the relevant transition-state energies may avoid the task of considering ground-state isomer interconversion and populations entirely” [20c].

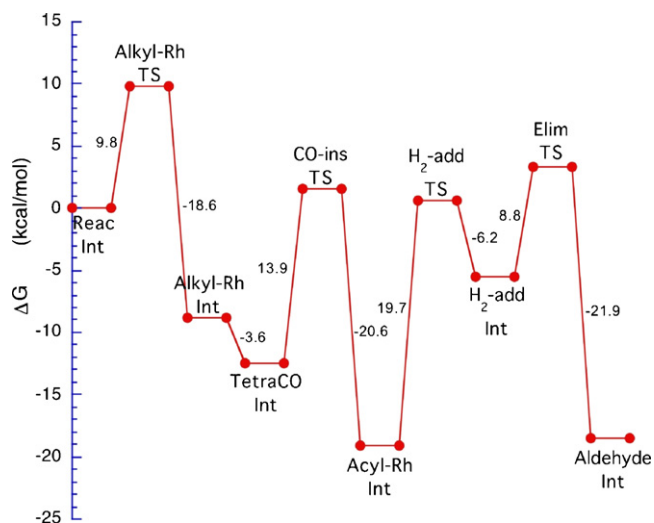


Fig. 4. Free energy profile along the L0 linear pathway for one of the **TMP₁** reactant intermediates. The CO addition TS cannot be located because, in the presence of CO, linear tricarbonyl intermediates directly evolve to tetracarbonyl intermediates.

2.3.1. Kinetic isotope effects

Despite the analogy found in the experimental runs between hydro- and deuterioformylations, the kinetic isotope effects (KIE) have been taken into account. In this case, KIE is given by:

$$\text{KIE} = \frac{k_{\text{H}}}{k_{\text{D}}}$$

where k_{H} and k_{D} are the reaction rate constants, computed via the Eyring–Polanyi equation [21]:

$$k = \left(\frac{k_{\text{B}}T}{h} \right) e^{-\Delta G^{\ddagger}/RT}$$

where k is the reaction rate constant, k_{B} the Boltzmann constant, T the absolute temperature, h the Planck's constant, ΔG^{\ddagger} the Gibbs free energy of activation, and R the gas constant.

To this aim, the free energies of all TS leading to the intermediates in Scheme 2 have been computed with the proper replacements of D to H: the differences are made with respect to the lowest free energy reactant intermediates taken as zero.³

When the isotopic substitution is in the chemical bond that is broken, i.e. in Rh–D as for the Rh–alkyl TS, the primary isotope effect is large ($1.69 \leq \text{KIE} \leq 1.71$ (for L regioisomers)), as expected. Conversely, the secondary kinetic isotope effect (SKIE), observed when D is contained in the alkyl part, not involved in bond breaking or forming events, is much smaller ranging from 0.36 (for L regioisomers) to 0.40. The velocity for the release of Rh–D is more than four times slower than that for the release of Rh–H, as pointed out in Section 3.

The results obtained for the monodeuterated TS are plotted in Fig. 5 as compared to those of the species containing only H atoms. From Fig. 5 it appears evident that the trend of hydroformylation and deuterioformylation is very similar. Of course, in the case of hydroformylation, the Rh–alkyl TS and the β -hydride elimination TS to return to the terminal olefin (i.e. the initial reactant intermediate) coincide, and thus they are displayed twice, perfectly aligned, in the plots. The TS for the release of D from the catalyst to the substrate is higher than that for the release of H from the substrate to the catalyst, as well known and noticed above. The different

behavior between branched and linear paths is striking. The linear conformers cannot give the internal olefin, and the TS for the migratory insertion of the alkyl onto the coordinated CO has a free energy comparable with that of the reactant intermediate (Fig. 5d). Concerning the branched conformers, only B0 yields the aldehyde (Fig. 5c) as the linear ones, whereas B'0 (Fig. 5b) β -eliminates producing the internal olefin, and B2 (Fig. 5a and Fig. 2) β -eliminates producing the terminal olefin.

2.3.2. Agostic interaction

The high barriers for the addition of the fourth CO group to the alkyl–Rh tricarbonyl intermediates along the branched profiles are due to the large stabilization of branched tricarbonyl intermediates when an agostic interaction is established between Rh and one of the nearby hydrogens. Examples of such interactions are shown in Fig. 6 for the B2 alkyl–Rh(CO)₃ intermediates deriving respectively from **TMP₁** and **DMP₁**. In the latter case, due to the H₃CCH_{iso} torsion, three conformers, named B2g, B2t, and B2g' are located. B2g' does not present however any agostic interaction because H_{iso} is farther apart from Rh (3.16 Å). The separations between Rh and the H in β are also displayed in each conformer, because they are important for the β -hydride elimination reaction to give the internal olefin.

Besides from geometrical parameters, reported in Table 4 (typically the distance between the metal (M) and the hydrogen is 1.8–2.3 Å and the M–H–C angle is 90–140°), this kind of interaction can be put forward from the existence of bond (BCP) and ring (RCP) critical points in Bader's topological analysis of the electron distribution [16]. The critical points involving Rh and the delocalization indices for the atoms bonded to Rh are reported in Tables 5 and 6. The graphical output obtained with AIMAll for tBu B'0 is displayed in Fig. S2 of ESI. From a perusal of Tables 4–6 it is evident that the agostic interactions (even those just outside the aforementioned distance limit) are confirmed by QTAIM that finds BCP and RCP with a significant density and delocalization index in all cases reported but iso B2g' and iso B'2g' (Figs. S3b,d–S4 of ESI), where the *i*Pr H (H_{iso}) points toward Rh instead of one of those belonging to its methyl groups (Fig. S5 of ESI).

It is noteworthy, however, that the behavior of this kind of systems is very similar at least concerning the agostic interaction. Furthermore, as already remarked, the approach of the fourth CO that might be hampered by a strong agostic interaction, shows lower TS than the alkyl migratory insertion onto the coordinated CO in any case.

2.3.3. Comparison between the hydroformylation behavior of **TMP₁** (tBu) and **DMP₁** (iso)

The free energy based L:B regioselectivity ratios computed for **TMP₁** and **DMP₁** under the hypothesis of nonreversibility (85:15 and 68:32, respectively) are significantly different, despite the similarity between the two substrates. The trivial reason for the computed ratios is that in the case of **DMP₁** there are 18 linear and 18 branched alkyl–Rh TS, whereas for **TMP₁** there are 6 linear and just 5 branched alkyl–Rh TS. The branched alkyl–Rh TS corresponding to the tBu–B2 alkyl–Rh(CO)₃ intermediate was not reachable from the tBu–B2 alkyl–Rh(CO)₃ intermediate, because invariably the TS optimization produced the tBu–B0 alkyl–Rh TS. Conversely, in an analogous run for **DMP₁**, even the critical B2g' alkyl–Rh TS and the relevant reactant intermediate have been obtained (Fig. 7). It is obvious that such structures are not attainable for **TMP₁**, owing to the steric hindrance of the tBu group.

In order to clarify matters, the subsequent reaction steps have been investigated also for **DMP₁** with a large computational effort

³ Reference free energies for Reac(H) and Reac(D) intermediates are –766.738577 and –766.741097 E_{h} , respectively. The free energy for CO is –113.560714 E_{h} .

Table 4
Geometrical parameters for some branched tricarbonyl intermediates of **TMP**₁ (tBu) and **DMP**₁ (iso).

	tBu B2	iso B2g	iso B2t	iso B2g'	tBu B'0	iso B'0t	iso B'0g	iso B'2g'	iso B0g'
Rh...H _β (Å)	2.4397	2.2909	2.3087	3.8769	2.1618	2.1945	2.4391	3.5000	2.5710
Rh...H...C (deg)	112.56	131.87	122.70	106.07	133.46	128.46	123.92	92.54	113.39

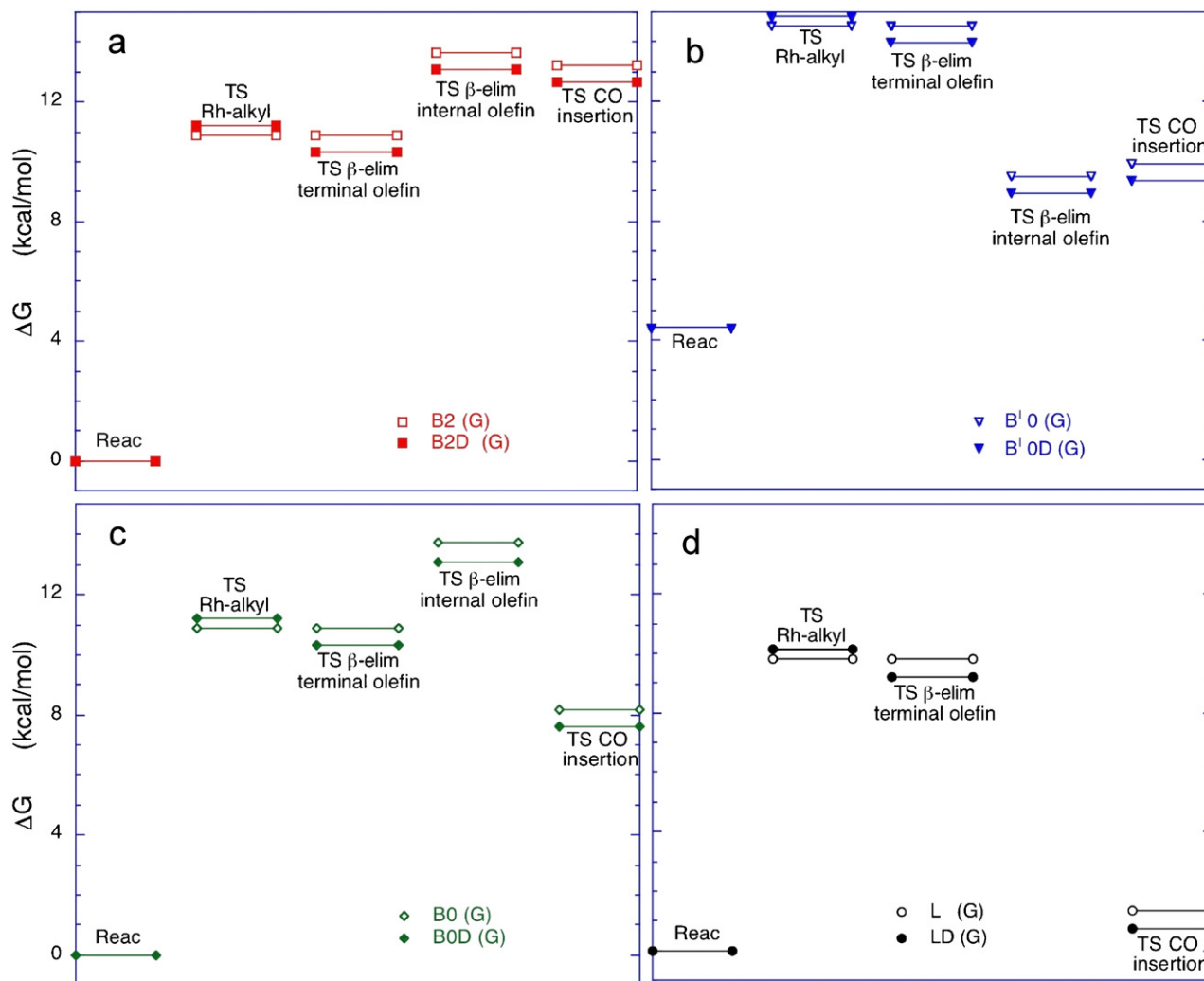


Fig. 5. TS free energies for a number of monodeuterated **TMP**₁ species (solid markers) in comparison to those of the corresponding non-deuterated species (empty markers): (a) B2D vs. B2; (b) B'0D vs. B'0; (c) B0D vs. B0; and (d) LD vs. L (all linear conformers show a very similar behavior); the lowest free energy reactant intermediates are taken as zero.

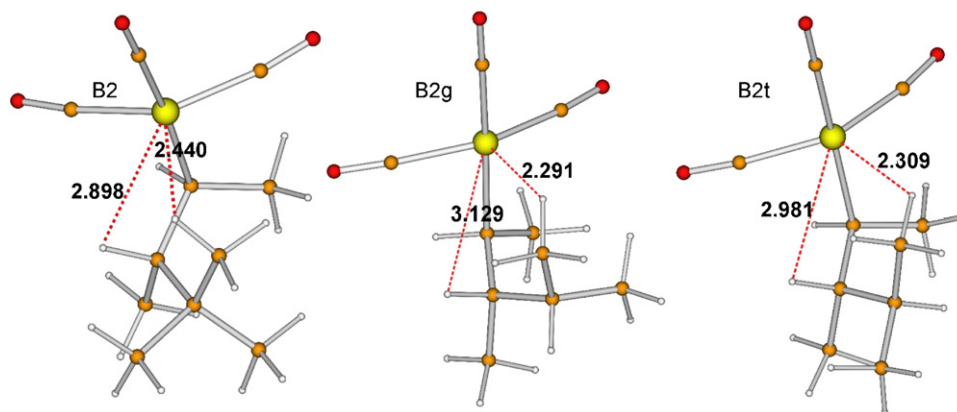


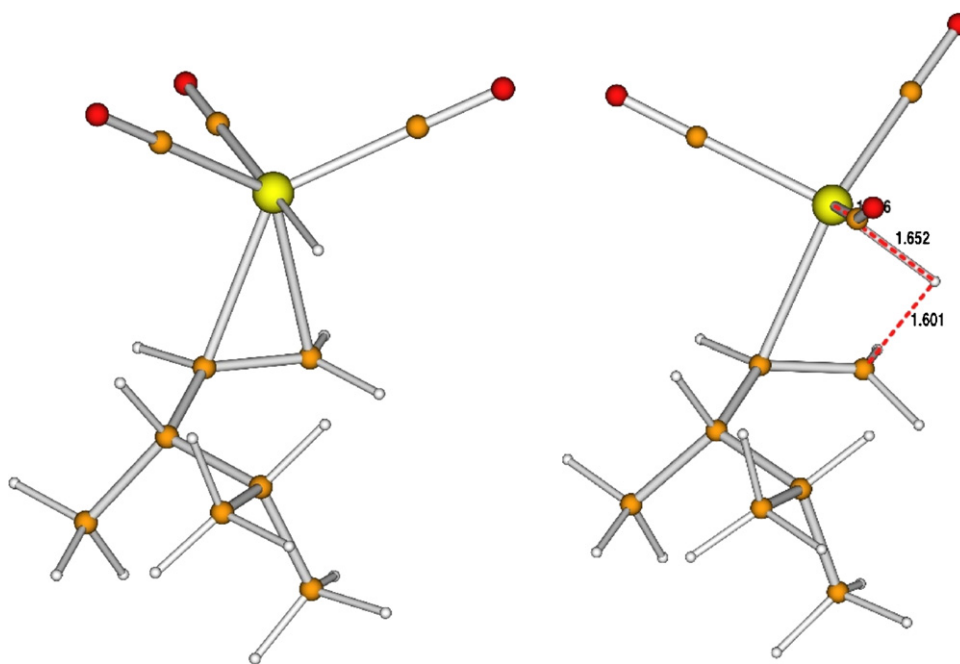
Fig. 6. Agostic interactions in branched tricarbonyl intermediates obtained for **TMP**₁ (B2) and **DMP**₁ (B2g and B2t). The separation between Rh and the H at the β carbon is also displayed. Distances in Å.

Table 5Electron density of bond (3, -1) and ring (3, +1) critical points for some branched tricarbonyl intermediates of **TMP**₁ (tBu) and **DMP**₁ (iso).

CP	tBu B2	iso B2g	iso B2t	iso B2g'	tBu B'O	iso B'Ot	iso B'Og	iso B'2g'	iso B0g'
C ₂ -Rh	0.1023	0.0999	0.1035	0.1020	0.0996	0.1011	0.0991	0.1041	0.0990
C ₄ -Rh	0.1252	0.1277	0.1243	0.1277	0.1279	0.1266	0.1291	0.1271	0.1294
C ₆ -Rh	0.1401	0.1388	0.1406	0.1403	0.1421	0.1411	0.1410	0.1432	0.1371
C ₈ -Rh	0.1408	0.1401	0.1410	0.1399	0.1357	0.1382	0.1368	0.1374	0.1403
H _a -Rh	0.0204	0.0262	0.0252	–	0.0336	0.0314	0.0203	–	0.0162
C ₂ -Rh-H _a -C ₂₁ -C ₂₀ -C ₁₄	0.0124	0.0108	0.0126	–	0.0122	0.0126	0.0170	–	0.0154

Table 6Delocalization index (DI(A,B)) of bonded atoms to Rh for some branched tricarbonyl intermediates of **TMP**₁ (tBu) and **DMP**₁ (iso).

CP	tBu B2	iso B2g	iso B2t	iso B2g'	tBu B'O	iso B'Ot	iso B'Og	iso B'2g'	iso B0g'
C ₂ -Rh	0.7876	0.7772	0.7946	0.7712	0.7617	0.7696	0.7536	0.7767	0.7528
C ₄ -Rh	1.0429	1.0636	1.0346	1.0699	1.0695	1.0583	1.0824	1.0652	1.0857
C ₆ -Rh	1.1058	1.0733	1.1048	1.0993	1.1086	1.1081	1.0864	1.1364	1.0593
C ₈ -Rh	1.1073	1.0941	1.1194	1.0979	1.0542	1.1082	1.0575	1.0919	1.0818
H _a -Rh	0.0878	0.1227	0.1071	–	0.1496	0.1374	0.0941	–	0.0721

**Fig. 7.** React2g' intermediate (left) and B2g' alkyl-Rh TS (right) obtained for **DMP**₁. Distances in Å.

due to the number of steps and of conformers.⁴ The relative free energy results for **DMP**₁ are reported in Table 7, limited to the most important TS⁵ relevant to reversibility. Analogous results for **TMP**₁ are reported in Table 8 for comparison.

In order to highlight the different behavior of 0-B2 and B2g' branched pathways for **TMP**₁ and **DMP**₁, respectively, the B2g' free energy profile for **DMP**₁ is shown in Fig. 8. In this case, both the Alkyl-Rh TS and the β-elim TS to yield the internal olefin are higher than the CO-ins TS. Therefore the branched pathway is

nonreversible and the branched aldehyde is produced opposite to what occurs for 0-B2 **TMP**₁.

The L0g' free energy profile for **DMP**₁, displayed in Fig. 9, closely resembles that for L0 **TMP**₁ shown in Fig. 4. Interested readers can find the **DMP**₁ structures in ESI (Figs. S6–S8).

From a perusal of Tables 7 and 8, it is indeed evident that all linear conformers proceed to give the aldehyde products. An analogous outcome is obtained for all the branched **DMP**₁ conformers. The branched **TMP**₁ conformers (Table 8) produce the branched aldehyde with the exception of B'O and B2 whose reaction is reversible: B'O undergoes β-hydride elimination to give the internal olefin, whereas B2 undergoes β-hydride elimination to return to the terminal olefin complex with the catalyst (see also Figs. 2 and 5), i.e. to the starting material. This reacts again going through the linear and branched paths with the original regioselectivity, therefore increasing the linear fraction. This explains the different behavior of **DMP**₁ and **TMP**₁.

Solvent (benzene) effects had been considered for **TMP**₁ [19] exploiting either the continuum solvent in the IEF-PCM framework [22] or the coordinating effect of a single solvent molecule. A

⁴ As mentioned above, there are 18 linear and 18 branched structures for each stationary point. A few constrained runs followed by a relaxed TS optimization are necessary for each TS. To locate the lowest free energy CO insertion TS the three equatorial CO groups need to be taken into account in turn also computing their vibrational frequencies.

⁵ For CO insertion TS, only the lowest free energy ones are reported. Concerning the reductive elimination to produce the aldehyde, only the B0 conformers have been reported because the free energy of that species in **TMP**₁ was higher than the TSinsCO one and close enough to the alkyl-Rh TS one.

Table 7
Relative free energies^a (kcal/mol) for a number of TS along the branched and linear pathways for the hydroformylation of **DMP**₁. Their imaginary frequencies (cm⁻¹) are also reported in parenthesis.

Conformer	Alkyl-Rh TS	CO-ins TS	Elim TS ^b	β-elim TS ^c (internal)
B2g	18.76 (716 i)	10.68 (214i)		12.63 (667i)
B2g'	13.02 (730 i)	7.71 (220i)	6.97 (723i)	8.70 (652i)
B2t	15.79 (737 i)	9.90 (204i)		13.68 (657i)
B0g	10.27 (685 i)	5.88 (219i)	7.53 (711i)	12.63 (667i)
B0g'	9.92 (698 i)	3.22 (226i)	4.80 (716i)	8.70 (652i)
B0t	10.77 (722 i)	6.48 (228i)	8.06 (715i)	13.68 (657i)
B1g	14.20 (701 i)	9.33 (184i)		
B1g'	14.04 (711 i)	7.41 (218i)		
B1t	12.02 (708 i)	5.89 (185i)		
B'2g	11.44 (743 i)	5.81 (244i)		7.58 (649i)
B'2g'	11.40 (711 i)	6.78 (222i)		8.96 (632i)
B'2t	12.22 (710 i)	5.84 (201i)		8.79 (645i)
B'0g	9.79 (695 i)	3.17 (215i)		7.58 (649i)
B'0g'	13.62 (700 i)	7.59 (199i)		8.96 (632i)
B'0t	14.08 (727 i)	– ^d		8.79 (645i)
B'1g	15.65 (701 i)	6.89 (192i)		
B'1g'	19.08 (708 i)	10.99 (177i)		
B'1t	15.82 (707 i)	8.82 (196i)		
L2g	16.07 (698i)	5.67 (240i)		
L2g'	12.08 (688i)	1.52 (252i)		
L2t	14.88 (664i)	2.86 (253i)		
L0g	10.15 (694i)	0.91 (273i)		
L0g'	9.49 (659i)	0.91 (272i)	3.42 (726i)	
L0t	9.98 (682i)	1.14 (263i)		
L1g	11.65 (645i)	4.20 (264i)		
L1g'	11.89 (660i)	4.04 (270i)		
L1t	10.80 (681i)	5.38 (258i)		
L'2g	10.42 (678i)	8.09 (241i)		
L'2g'	10.24 (681i)	8.22 (241i)		
L'2t	10.79 (666i)	2.54 (272i)		
L'0g	9.69 (643i)	1.54 (274i)		
L'0g'	11.52 (651i)	1.46 (262i)		
L'0t	11.97 (654i)	1.46 (274i)		
L'1g	13.37 (620i)	2.48 (274i)		
L'1g'	16.01 (664i)	3.06 (266i)		
L'1t	14.04 (657i)	3.09 (264i)		

^a Reference free energies are: $\text{Reac Int} = -727.307455E_h$, $\text{Reac Int} + \text{CO} = -840.868169E_h$, $\text{Reac Int} + \text{CO} + \text{H}_2 = -842.080705E_h$.^b Reductive elimination TS to produce aldehyde intermediates have been computed just for critical cases, when possibly competitive with relatively low alkyl-Rh TS.^c While B1 and B'1 cannot β-eliminate as such because their H₃ is on the opposite side with respect to Rh, B2 and B0 yield the same internal olefin, in analogy to B'2 and B'0, because their H₃ move (from gauche⁻ and t) to a syn position with respect to Rh. Linear isomers cannot give the internal olefin via β-elimination, because Rh is on the first C.^d The relaxed TS optimizations invariably return to a tetracarbonyl intermediate structure with a rotated methyl group.

negligible effect on structure and free energies was observed in the case of PCM, as expected, due to the small difference between benzene ($\epsilon = 2.247$) and vacuum dielectric constants. On the other hand, in the supermolecule approach, the TS free energy gap remained unaltered upon inclusion of a benzene molecule that did not affect the mutual position of the various TS.

3. Experimental

Benzene was dried over molecular sieves and distilled under nitrogen. Rh₄(CO)₁₂ was from Strem products. The starting olefins (3-methylbut-1-ene and 3-methylpent-1-ene) were commercially available. NMR spectra were recorded on a Varian Gemini 200 MHz

Table 8
Relative free energies^a (kcal/mol) for a number of TS along the branched and linear pathways for the hydroformylation of **TMP**₁. Their imaginary frequencies (cm⁻¹) are also reported in parenthesis.

Conformer	Alkyl-Rh TS	CO-ins TS	Elim TS	β-elim TS ^b (internal)
O-B2	10.88 (689i)	13.24 (212i)	10.56 (737i)	13.66 (680i)
B0	10.88 (689i)	8.16 (209i)	9.66 (710i)	13.72 (685i)
B1	15.02 (702i)	9.47 (179i)	7.60 (735i)	–
B'2	11.69 (720i)	7.41 (227i)	6.83 (705i)	9.48 (630i)
B'0	14.52 (697i)	9.91 (190i)	8.32 (706i)	9.48 (630i)
B'1	18.53 (721i)	11.70 (173i)	14.02 (719i)	–
L2	17.61 (684i)	2.73 (277i)	6.16 (714i)	–
L0	9.80 (682i)	1.36 (265i)	3.31 (718i)	–
L1	12.41 (645i)	4.41 (265i)	6.02 (716i)	–
L'2	10.90 (679i)	1.20 (277i)	2.76 (720i)	–
L'0	13.03 (651i)	2.14 (262i)	4.21 (719i)	–
L'1	17.98 (554i)	4.48 (273i)	5.72 (725i)	–

^a Reference free energies are: $\text{Reac Int} = -766.738577E_h$, $\text{Reac Int} + \text{CO} = -880.299291E_h$, $\text{Reac Int} + \text{CO} + \text{H}_2 = -881.511827E_h$.^b While B1 and B'1 cannot β-eliminate as such because their H₃ is on the opposite side with respect to Rh, B2 and B0 yield the same internal olefin, in analogy to B'2 and B'0, because their H₃ move (from gauche⁻ and t) to a syn position with respect to Rh. Linear isomers cannot give the internal olefin via β-elimination, because Rh is on the first C.

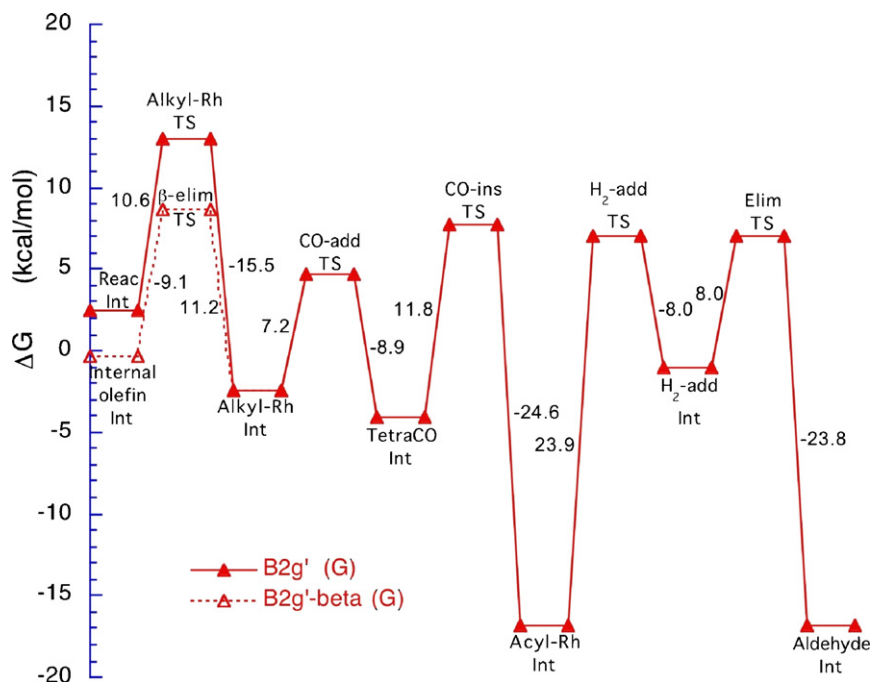


Fig. 8. Free energy profile along the B2g' branched pathway for **DMP₁** corresponding to the 0-B2 for **TMP₁**. The β -elimination TS leading to the internal olefin is drawn with dotted lines and empty markers.

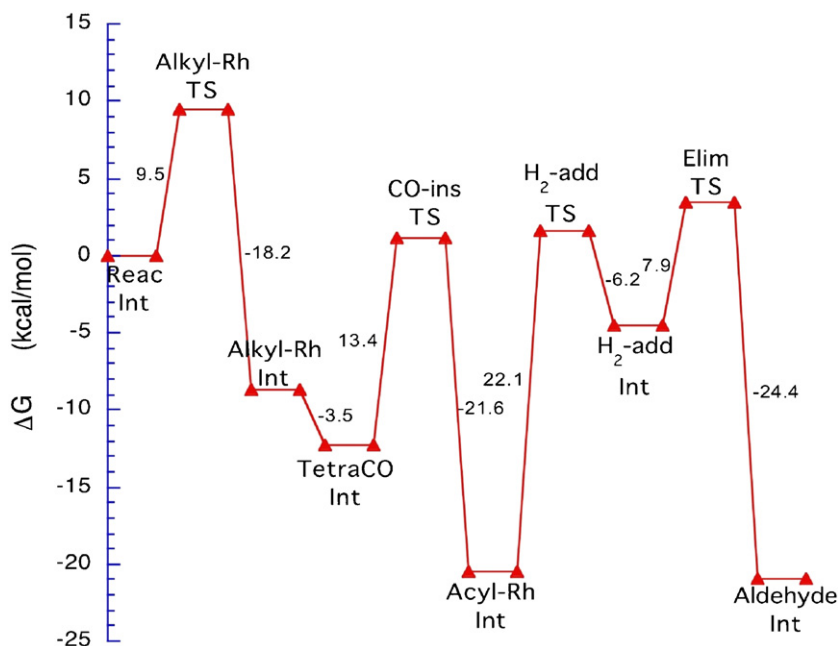


Fig. 9. Free energy profile along the L0g' linear pathway for one of the **DMP₁** reactant intermediates (Reac0g').

and on a Varian Gemini 300 MHz using benzene-*d*₆ as solvent. GC analysis was carried out on a Perkin Elmer 8600 gas chromatograph, using a BP1 column (15 m × 0.32 mm × 0.25 μ m), using helium as carrier gas.

3.1. Hydroformylation or deuteroformylation of 3,4,4-trimethylpent-1-ene (**TMP₁**): general procedure

A solution of 3,4,4-trimethylpent-1-ene (2.78 mmol) and Rh₄(CO)₁₂ (Rh/substrate = 1/1000) in benzene (5 ml) was introduced by suction into an evacuated 25 ml stainless steel autoclave. Carbon monoxide was introduced, the autoclave was then rocked

and hydrogen or deuterium was rapidly introduced up to 100 atm total pressure (CO/H₂(D₂) = 1:1). When the gas absorption reached the value corresponding to the fixed conversion, the reaction mixture was siphoned out. The degree of conversion was measured by GLC, using n-decane as the internal standard.

4. Computational details

The Rh-carbonyl hydride [H–Rh(CO)₃], produced by the unmodified catalytic precursor [Rh₄(CO)₁₂] under mild hydroformylation conditions, is the catalytic active species used to study the reaction regioselectivity (L:B, Scheme 1). Since the reaction occurs at rt, a

consistent comparison between theoretical and experimental values can be performed, as we demonstrated in our first study on the hydroformylation regioselectivity [13a] for a series of eight mono-substituted olefins plus ethene and dimethylethene. Because for nonreversible reactions the olefin insertion into the Rh–H bond turned out to be the step determining the regioselectivity,⁶ in the computational strategy employed, the L:B regioisomeric ratio was theoretically evaluated exploiting the free energy differences that can be approximated by the potential energy differences, of branched and linear alkyl–rhodium transition states, using the formula:

$$L : B = k_L : k_B = \frac{\sum e^{-\Delta G_L^\ddagger / RT}}{\sum e^{-\Delta G_B^\ddagger / RT}} \approx \frac{\sum e^{-\Delta E_L^\ddagger / RT}}{\sum e^{-\Delta E_B^\ddagger / RT}} \quad (1)$$

where k is the reaction rate, ΔG^\ddagger and ΔE^\ddagger are the relative TS free energies and potential energies with respect to the most stable TS. Zero-point vibrational energies and thermal corrections were computed in the rigid rotor-harmonic oscillator approximation to obtain the free energies [23] at 298.15 K. The summations run over all the possible branched and linear alkyl–Rh TS structures.

Density functional theory (DFT) calculations have been carried out with the Gaussian 03 suite of codes [24], using for C, O, and H the Becke gradient-corrected three-parameter hybrid exchange and Perdew 86 gradient-corrected correlation functionals, i.e. B3P86 [25,26], and the 6-31G* basis set [27]. Effective core potentials (implicitly including some relativistic effects for the electrons near the nucleus), coupled to the LanL2DZ valence basis set, have been used for Rh [28].

Due to the conformational flexibility of 1-alkenes, a variety of reactant complexes with H–Rh(CO)₃ must be considered to explore the reaction mechanism. For alkyl–Rh TS all rotamers need to be taken into account although only those within ~5 kcal/mol of the most favorable one are included into Eq. (1) to evaluate the regioselectivity [13]. Branched and linear pathways must be followed for each conformer when subsequent reaction steps are examined, because it is difficult to model build from scratch likely TS structures. Several constrained optimizations in the TS region are necessary that are eventually relaxed employing TS optimizations. In few cases however it was impossible to obtain the sought TS structures despite a number of trials, because TS optimizations lead to rotational TS of nearby intermediates.

QTAIM calculations have been carried out with AIMAll [29]. Structures and normal modes have been visualized using Molden [30].

5. Conclusions

It is well documented [7] that the olefin structure plays an important role in the reaction regioselectivity. The branched isomer is remarkably more favored when vinyl aromatic substrates, such as vinylpyrrole, vinylstyrene, or vinylpyridine, are taken into account. The branched isomer also prevails in the hydroformylation of vinyl allyl ethers. In the case of the alkyl vinyl and alkyl allyl substrates both regioisomers are formed in a very similar amount.

In order to evaluate how the steric hindrance due to a sec-alkyl group bonded to the vinyl group can affect the β -regioselectivity of the reaction, the hydroformylation of four substrates (3-methylbut-1-ene (**MB**₁), 3-methylpent-1-ene (**MP**₁), 3,4-dimethylpent-1-ene (**DMP**₁), and 3,4,4-trimethylpent-1-ene (**TMP**₁)), characterized by an increasing steric hindrance of the group bonded to the vinyl

group was carried out. In all cases the linear isomer prevails with respect to the branched one in the 2:1 ratio or more. An anomalous behavior is found for **TMP**₁ (R = tBu), where the linear isomer largely prevails (L:B = 95:5). A profound examination of the reaction course via deuterioformylation experiments (carried out at partial substrate conversion as well) showed that the alkyl–rhodium formation resulted to be irreversible for all substrates except for the bulkier one (**TMP**₁). In that particular case, a significant amount of β -elimination was observed but only for the branched alkyl isomer. This fact explains the high selectivity in favor of the linear aldehyde because, while the linear alkyl proceeds toward the aldehyde, the branched alkyl primarily undergoes β -elimination and only in a very limited amount is transformed into the related aldehyde. It should be noted that the ²H NMR analysis of the crude deuterioformylation reaction mixture is a direct and simple method to investigate the different nature and fate of the alkyl–metal intermediates [3,7,8,31–34].

Theoretical calculations on the regioselectivity of the alkyl–metal intermediates formation show a good agreement with regioselectivity values experimentally determined on the aldehyde. Only in the case of **TMP**₁, the theoretical values of regioselectivity (L:B = 85:15), calculated under the hypothesis of nonreversibility, are slightly underestimated with respect to the experimental values (L:B = 95:5). Interestingly, the careful analysis of the branched pathway put forward a free energy transition state (TS) for the migratory insertion of the alkyl onto the Rh-coordinated CO higher than the alkyl–Rh formation TS thus preventing the branched aldehyde formation. In such a case, the reaction moves backwards, producing again the initial olefin complex (corresponding to the monodeuterated **TMP**₁-1-*d*₁ species obtained in deuterioformylation experiments at partial substrate conversion) and enriching the linear fraction that invariably proceeds to aldehyde. An analogous analysis carried out for **DMP**₁ puts forward a nonreversible mechanism for every conformer and points out that the steric hindrance of the tBu group hampers the attainment of the B2 alkyl–Rh TS for **TMP**₁ favoring the initial olefin complex formation for that conformer.

Therefore, although the steric hindrance was expected to influence the reaction, it was however difficult to understand how and where from the experiment. While deuterioformylation runs are useful to show that β -hydride elimination occurs, only the theoretical inspection explains at which step of the reaction this happens.

This investigation clearly illustrates how important (perhaps fundamental) is to tackle regioselectivity issues in hydroformylation reactions using different and complementary approaches, such as deuterioformylations and theoretical calculations, because together they permit a better understanding and a proper interpretation of the mechanism of this significant reaction which despite over 60 years old becomes more and more beautiful and intriguing.

Acknowledgments

R.L. and R.S. are indebted to Prof. Aldo Vitagliano for supplying the 3,4-dimethylpent-1-ene and 3,4,4-trimethylpent-1-ene samples. G.A. and C.G. are grateful to Todd A. Keith for practical advice and helpful comments on the treatment of ECP-modeled core electrons in AIMAll.

Appendix A. Supplementary data

Supplementary data associated with this article can be found, in the online version, at doi:10.1016/j.molcata.2011.12.021.

⁶ That step can determine also the diastereoselectivity as in vinyl olefins containing chiral alkoxy or alkyl groups [13b].

References

- [1] R. Lazzaroni, R. Settambolo, G. Uccello-Barretta, *Organometallics* 14 (1995) 4644–4650.
- [2] (a) B.E. Hanson, N.E. Davis, *J. Chem. Educ.* 64 (1987) 928–931;
(b) R. Lazzaroni, P. Pertici, S. Bertozzi, G. Fabrizi, *J. Mol. Catal.* 58 (1990) 75–85.
- [3] R. Lazzaroni, G. Uccello-Barretta, M. Benetti, *Organometallics* 8 (1989) 2323–2327.
- [4] I. Ojima, *Chem. Rev.* 88 (1988) 1011–1030.
- [5] (a) P. Kalck, F. Serein-Spirau, *New J. Chem.* 13 (1989) 515–518;
(b) A.L. Lapidus, A.P. Rodin, I.G. Pruidze, B.I. Ugrak, *Izv. Akad. Nauk SSSR, Ser. Khim* 7 (1990) 1661–1662.
- [6] A.F. Browning, A.D. Bacon, C. White, D.J. Milner, *J. Mol. Catal.* 83 (1993) L11–L14.
- [7] R. Lazzaroni, R. Settambolo, A. Caiazzo, in: P.W.N.M. van Leeuwen, C. Claver (Eds.), *Rhodium Catalyzed Hydroformylation*, Kluwer, Dordrecht, 2000, Chapter 2.
- [8] R. Settambolo, S. Scamuzzi, A. Caiazzo, R. Lazzaroni, *Organometallics* 17 (1998) 2127–2130.
- [9] A. Caiazzo, R. Settambolo, L. Pontorno, R. Lazzaroni, *J. Organomet. Chem.* 599 (2000) 298–303.
- [10] C.P. Casey, L.M. Petrovich, *J. Am. Chem. Soc.* 117 (1995) 6007–6014.
- [11] N. Sakai, S. Mano, K. Nozaki, H. Takaya, *J. Am. Chem. Soc.* 115 (1993) 7033–7034.
- [12] K. Nozaki, N. Sakai, T. Nanno, T. Higashijima, S. Mano, T. Horiuchi, H. Takaya, *J. Am. Chem. Soc.* 119 (1997) 4413–4423.
- [13] (a) G. Alagona, C. Ghio, R. Lazzaroni, R. Settambolo, *Organometallics* 20 (2001) 5394–5404;
(b) G. Alagona, C. Ghio, R. Lazzaroni, R. Settambolo, *Inorg. Chim. Acta* 357 (2004) 2980–2988.
- [14] G. Alagona, R. Lazzaroni, C. Ghio, *J. Mol. Model.* 17 (2011) 2275–2284.
- [15] (a) H.C. Urey, D. Rittenberg, *J. Chem. Phys.* 1 (1933) 137–143;
(b) J. Bigeleisen, M.G. Mayer, *J. Chem. Phys.* 15 (1947) 261–267;
(c) J. Evans, J. Schwartz, P.W. Urquhart, *J. Organomet. Chem.* 81 (1974) C37.
- [16] R.F.W. Bader, *Atoms in Molecules: A Quantum Theory*, Oxford University Press, Oxford, 1990.
- [17] C. Ghio, R. Lazzaroni, G. Alagona, *Eur. J. Inorg. Chem.* (2009) 98–103.
- [18] R. Lazzaroni, R. Settambolo, G. Alagona, C. Ghio, *Coord. Chem. Rev.* 254 (2010) 696–706.
- [19] G. Alagona, C. Ghio, *Theor. Chem. Acc.*, in press.
- [20] (a) D.Y. Curtin, *Rec. Chem. Prog.* 15 (1954) 111–128;
(b) L.P. Hammett, *Physical Organic Chemistry*, 2nd edn., McGraw-Hill, New York, 1970, pp. 119–120, Chapter 5;
(c) J.I. Seeman, *Chem. Rev.* 83 (1983) 84–134.
- [21] (a) H. Eyring, *J. Chem. Phys.* 3 (1935) 107–115;
(b) M.G. Evans, M. Polanyi, *Trans. Faraday Soc.* 31 (1935) 875–894.
- [22] (a) S. Miertus, E. Scrocco, J. Tomasi, *Chem. Phys.* 55 (1981) 117–129;
(b) S. Miertus, J. Tomasi, *Chem. Phys.* 65 (1982) 239–245;
(c) J. Tomasi, M. Persico, *Chem. Rev.* 94 (1994) 2027–2094;
(d) J. Tomasi, B. Mennucci, E. Cancès, *J. Mol. Struct. Theochem.* 464 (1999) 211–226;
(e) J. Tomasi, B. Mennucci, R. Cammi, *Chem. Rev.* 105 (2005) 2999–3094.
- [23] D.A. McQuarrie, *Statistical Mechanics*, University Science Book, Sausalito, CA, 2000.
- [24] M.J. Frisch, G.W. Trucks, H.B. Schlegel, G.E. Scuseria, M.A. Robb, J.R. Cheeseman, J.A. Montgomery Jr., T. Vreven, K.N. Kudin, J.C. Burant, J.M. Millam, S.S. Iyengar, J. Tomasi, V. Barone, B. Mennucci, M. Cossi, G. Scalmani, N. Rega, G.A. Petersson, H. Nakatsuji, M. Hada, M. Ehara, K. Toyota, R. Fukuda, J. Hasegawa, M. Ishida, T. Nakajima, Y. Honda, O. Kitao, H. Nakai, M. Klene, X. Li, J.E. Knox, H.P. Hratchian, J.B. Cross, V. Bakken, C. Adamo, J. Jaramillo, R. Gomperts, R.E. Stratmann, O. Yazyev, A.J. Austin, R. Cammi, C. Pomelli, J.W. Ochterski, P.Y. Ayala, K. Morokuma, G.A. Voth, P. Salvador, J.J. Dannenberg, V.G. Zakrzewski, S. Dapprich, A.D. Daniels, M.C. Strain, O. Farkas, D.K. Malick, A.D. Rabuck, K. Raghavachari, J.B. Foresman, J.V. Ortiz, Q. Cui, A.G. Baboul, S. Clifford, J. Cioslowski, B.B. Stefanov, G. Liu, A. Liashenko, P. Piskorz, I. Komaromi, R.L. Martin, D.J. Fox, T. Keith, M.A. Al-Laham, C.Y. Peng, A. Nanayakkara, M. Challacombe, P.M.W. Gill, B. Johnson, W. Chen, M.W. Wong, C. Gonzalez, J.A. Pople, *Gaussian 03, Revision C. 02*, Gaussian Inc, Wallingford, CT, 2004.
- [25] A.D. Becke, *J. Chem. Phys.* 98 (1993) 5648–5652.
- [26] J.P. Perdew, *Phys. Rev. B* 33 (1986) 8822–8824.
- [27] W.J. Hehre, L.P. Radom, P.v.R. Schleyer, J.A. Pople, *Ab Initio Molecular Orbital Theory*, Wiley, New York, 1986.
- [28] P.J. Hay, W.R. Wadt, *J. Chem. Phys.* 82 (1985) 270–283.
- [29] Molden (Version 4.8), G. Schaftenaar, J.H. Noordik, *J. Comput. Aided Mol. Des.* 14 (2000) 123–134.
- [30] T.A. Keith, *AIMAll* (Version 11.10.16), TK Gristmill Software, Overland Park, KS, USA, 2011 (aim.tkgristmill.com).
- [31] G. Uccello-Barretta, R. Lazzaroni, R. Settambolo, P. Salvadori, *J. Organomet. Chem.* 417 (1991) 111–119.
- [32] R. Lazzaroni, R. Settambolo, A. Caiazzo, M. Bennett, *Organometallics* 21 (2002) 2454–2459.
- [33] R. Lazzaroni, R. Settambolo, G. Prota, C. Botteghi, S. Paganelli, M. Marchetti, *Inorg. Chim. Acta* 357 (2004) 3079–3083.
- [34] R. Lazzaroni, R. Settambolo, M. Marchetti, S. Paganelli, G. Alagona, C. Ghio, *Inorg. Chim. Acta* 362 (2009) 1641–1644.
- [35] D. Evans, J.A. Osborn, G. Wilkinson, *J. Chem. Soc. A* (1968) 3133–3142.